MULTISPECTRAL DEMOSAICKING WITH NOVEL GUIDE IMAGE GENERATION AND RESIDUAL INTERPOLATION

Yusuke Monno[1]*, Daisuke Kiku*[1]*, Sunao Kikuchi* [2]*, Masayuki Tanaka*[1]*, and Masatoshi Okutomi* [1]

[1] Tokyo Institute of Technology, Tokyo, Japan [2] Olympus R&D Center, Tokyo, Japan

ABSTRACT

A one-shot multispectral imaging system using a multispectral filter array (MSFA) provides a practical solution for compact, low-cost, and real-time multispectral imaging. However, multispectral demosaicking is a challenging problem because each spectral band is significantly undersampled in the MSFA. In this paper, we propose a novel demosaicking algorithm for the MSFA proposed in [1, 2]. Main contributions of this paper are (i) we utilize multispectral correlations for generating a guide image, which is effectively used for interpolation preserving image structures, and (ii) we effectively use residual interpolation (RI) [3] for generating the guide image and interpolating each spectral band. Experimental results demonstrate that our proposed algorithm significantly outperforms existing state-of-the-art algorithms.

Index Terms— Demosaicking, interpolation, multispectral filter array, multispectral imaging, spectral correlation.

1. INTRODUCTION

Multispectral imaging with more than three spectral bands can offer accurate spectral information of a captured scene. This spectral information is very useful for a wide field of computer vision and image processing applications such as relighting [4, 5] and segmentation in the spectral domain [6].

In the past few decades, many multispectral imaging systems have been proposed (e.g., [4–9]). However, in practical use, these systems still have limitations in terms of size, cost, and real-time imaging due to the requirement of multiple cameras [7], multiple shots [8], a high-speed lighting system [4, 5], or a special optical element such as a prism [6] and a diffraction grating [9].

One practical solution for compact, low-cost and real-time multispectral imaging is an extension of a commonly used color filter array (CFA) to a multispectral filter array (MSFA), in which more than three spectral bands are subsampled [1, 2, 10–15]. However, multispectral demosaicking, which is an interpolation process of the subsampled spectral bands, is a challenging problem because each spectral band is significantly undersampled in the MSFA due to the increasing number of spectral bands. Although many sophisticated demosaicking algorithms have been proposed [16, 17] for the most popular Bayer CFA [18], only a few algorithms have addressed the multispectral demosaicking problem [1, 2, 11, 12].

In this paper, we propose a novel multispectral demosaicking algorithm for the MSFA recently proposed in [1, 2]. We improve the previous algorithms [1, 2] in the following two points: (i) We propose a novel guide image generation algorithm utilizing multispectral correlations. (ii) We use residual interpolation (RI) [3] for generating the guide image and interpolating each subsampled spectral band. Experimental results demonstrate that our proposed algorithm significantly outperforms existing state-of-the-art algorithms.

2. PROPOSED ALGORITHM

2.1. Overview

Fig. 1 (a) and (b) show the five band MSFA and its schematic spectral sensitivities recently proposed in [1, 2]. Fig. 1 (c) shows the overall flow of our proposed demosaicking algorithm. We first subsample the MSFA RAW data into the five bands, which are referred to as subsampled R, Or, G, Cy, and B band data respectively.

Then, we follow the previous framework [1, 2] and interpolate the subsampled G band data to generate the guide G image, which is effectively used for the following interpolation as a reference to exploit image structures. The key of this framework is to generate an effective guide image which preserves edges and textures. This is the reason why the G band has the sampling density as high as the Bayer CFA, from which the guide image is generated.

In the previous algorithms [1,2], the missing guide G pixel values are interpolated by a weighted average of only subsampled G band data. However, many of existing Bayer demosaicking algorithms have proved the effectiveness of the interpolation in a color difference domain assuming an interband spectral correlation [16, 17]. Recently, we also proposed more powerful residual interpolation (RI) [3], which performs the interpolation in a residual domain rather than the color difference domain. Based on this fact, we utilize the RI for guide generation (GG) assuming multispectral correlations. For example, the guide G pixel values at R pixels are interpolated in the residual domain assuming the spectral correlation between the G band and the R band (GG at R in Fig. 1). The spectral correlations between the G band and the other bands

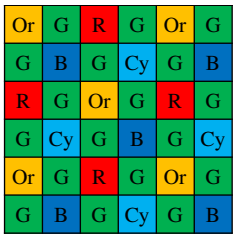

(a) MSFA

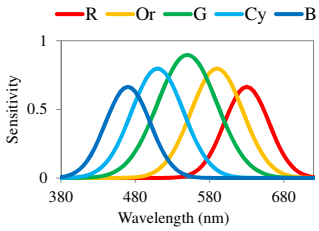

(b) Schematic spectral sensitivities

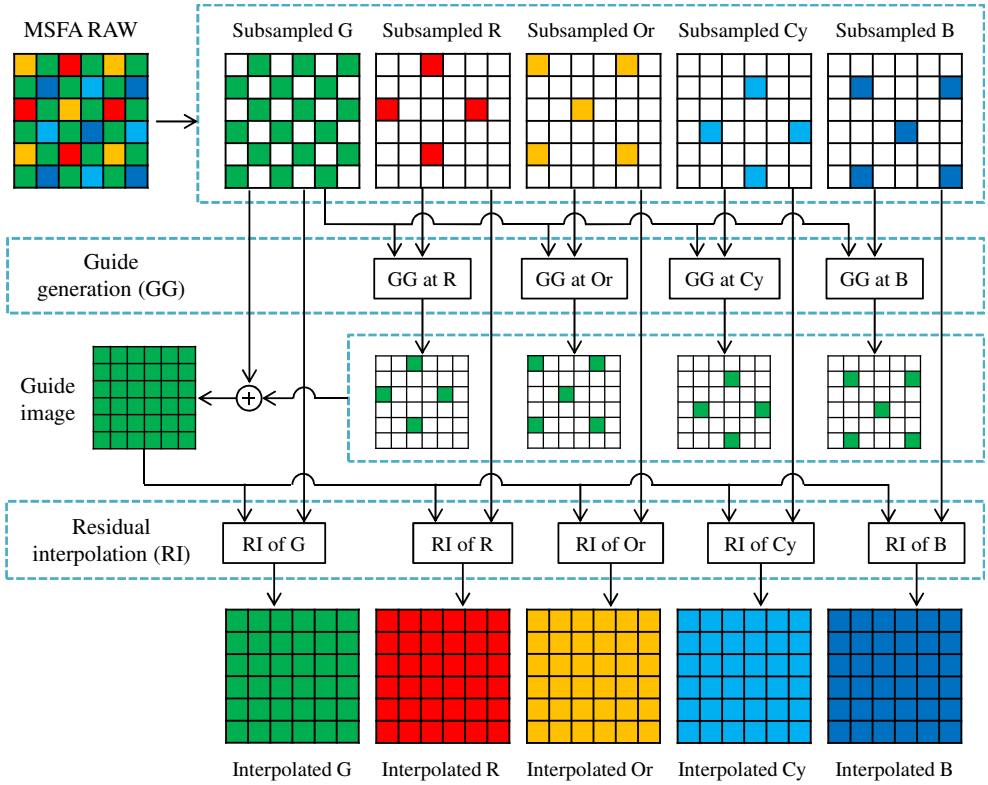

(c) Overall flow of our proposed algorithm.

Fig. 1. (a) MSFA, (b) schematic spectral sensitivities of each spectral band, and (c) overall flow of our proposed algorithm.

are similarly used. The interpolated G pixel values at all pixels are merged to compose the guide G image.

Finally, we interpolate each subsampled five band data by guided upsampling using the generated guide G image. For this upsampling, we utilize the RI again, which can improve the performance compared to the joint bilateral filter [19] and the guided filter (GF) [20] previously used in [1, 2].

2.2. Guide image generation

In this subsection, we describe the detail of the GG using multispectral correlations and the RI [3]. Fig. 2 shows the GG at the R pixels in Fig. 1 using the spectral correlation between the G band and the R band.

The GG at the R pixels consists of the following four steps: (i) Horizontal and vertical interpolations are applied to the sabsampled G and R band data to generate horizontally and vertically interpolated G and R band data. We utilize the RI in this step. (ii) Horizontal and vertical color differences (G-R) are calculated. (iii) The horizontal and vertical color differences are smoothed and combined into the final color difference estimates at the R pixels. (iv) The G pixel values at the R pixels are interpolated by adding the subsampled R band data to the final color difference estimates. We describe the details of each step in the following.

Fig. 3 shows the horizontal interpolation of the sabsampled R band data by the RI in the step (i). In the horizontal RI of the sabsampled R band data, horizontal linear interpolation is first applied to the subsmpled G band data at the rows that exist R pixels (R rows in Fig. 2) as: $\hat{G}^H_{i,j} = (G_{i,j-1} + G_{i,j+1})/2$, where i, j represents an interpolated pixel index. The key of the RI is to generate tentative estimates $\check{\mathrm{R}}^{\mathrm{H}}$ of R pixel values and calculate residuals $(\mathrm{R} - \check{\mathrm{R}}^{\mathrm{H}})$, instead of color differences. This residual transformation makes the interpolation process more precise than the standard color difference transformation. The tentative estimates are estimated by guided upsampling using the horizontally interpolated $\hat{\mathrm{G}}^{\mathrm{H}}$ as a guide. We simply use the GF [20] for the guided upsampling. After the tentative estimates generation, residuals are calculated and the horizontal linear interpolation of the residuals is performed. Finally, the tentative estimates are added to the interpolated residuals to obtain horizontally interpolated R band data $\tilde{R}^H$. The horizontal RI of the subsampled G and the vertical RI of the subsampled R and G are similarly performed.

In the step (ii), horizontal and vertical color differences are calculate as:

$$\tilde{\Delta}^H_{g,r}(i,j) = \begin{cases} \tilde{G}^H_{i,j} - R_{i,j}, & \text{G is interpolated} \\ G_{i,j} - \tilde{R}^H_{i,j}. & \text{R is interpolated} \end{cases}$$
$$\tilde{\Delta}^V_{g,r}(i,j) = \begin{cases} \tilde{G}^V_{i,j} - R_{i,j}, & \text{G is interpolated} \\ G_{i,j} - \tilde{R}^V_{i,j}. & \text{R is interpolated} \end{cases} \quad (1)$$

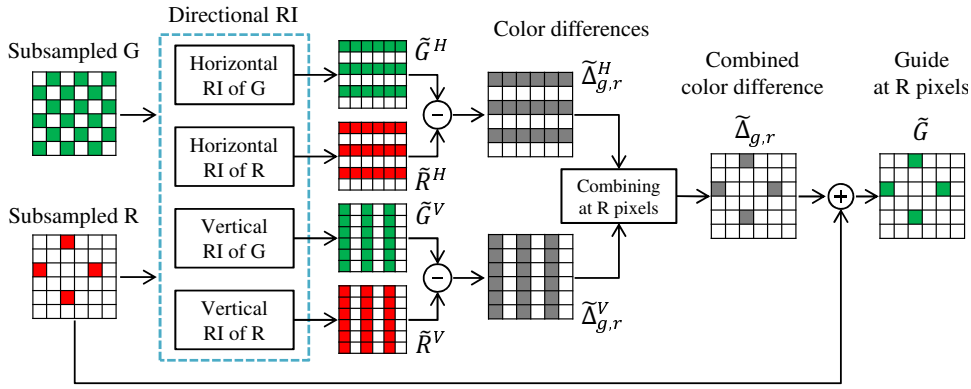

Fig. 2. Flowchart of the GG at the R pixels. The GG at the other pixels is similarly performed.

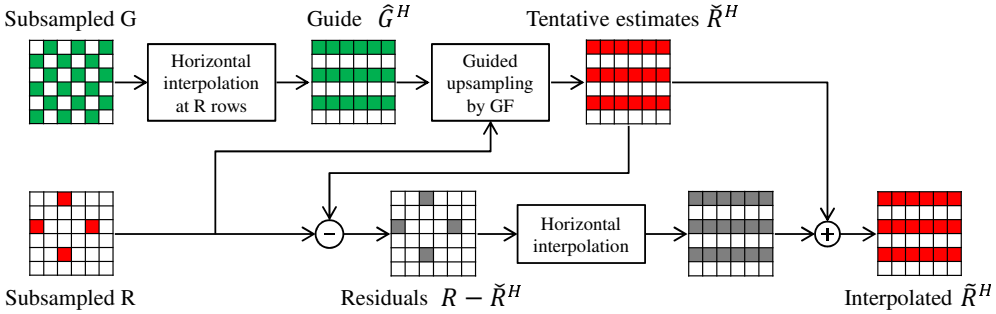

Fig. 3. Flowchart of the horizontal RI of the subsampled R band data in Fig. 2. The horizontal RI of G, the vertical RI of R, and the vertical RI of G are similarly performed.

Then, in the step (iii), the horizontal and vertical color differences are smoothed and combined as:

$$\begin{aligned}\tilde{\Delta}_{g,r}(i,j) = \{&\omega_N * f_{NE} * \tilde{\Delta}^V_{g,r}(i-3:i,j)+\\ &\omega_S * f_{SW} * \tilde{\Delta}^V_{g,r}(i:i+3,j)+\\ &\omega_E * \tilde{\Delta}^H_{g,r}(i,j-3:j) * f^T_{NE}+\\ &\omega_W * \tilde{\Delta}^H_{g,r}(i,j:j+3) * f^T_{SW}\}/\omega_T,\end{aligned} \tag{2}$$

where

$$\begin{aligned}\omega_T &= \omega_N + \omega_S + \omega_E + \omega_W,\\ f_{NE} &= [0.01, 0.08, 0.35, 0.56],\\ f_{SW} &= [0.56, 0.35, 0.08, 0.01],\end{aligned} \tag{3}$$

f_{NE}, and f_{SW} are Gaussian weighted averaging filters. We empirically used 1 for the standard deviation of the Gaussian weight. The weights for each direction $(\omega_N, \omega_S, \omega_E, \omega_W)$ are calculated using color difference gradients of all spectral bands in the horizontal and vertical directions as:

$$\begin{aligned}\omega_N &= 1/\left(\sum_{a=i-3}^{i}\sum_{b=j-2}^{j+2} D^V_{a,b}\right)^2, \omega_S = 1/\left(\sum_{a=i}^{i+3}\sum_{b=j-2}^{j+2} D^V_{a,b}\right)^2,\\ \omega_E &= 1/\left(\sum_{a=i-2}^{i+2}\sum_{b=j}^{j+3} D^H_{a,b}\right)^2, \omega_W = 1/\left(\sum_{a=i-2}^{i+2}\sum_{b=j-3}^{j} D^H_{a,b}\right)^2,\end{aligned} \tag{4}$$

where the directional color difference gradients are calculated as:

$$\begin{aligned}D^H_{i,j} &= \sum_{c\in\{r,or,cy,b\}} \|\tilde{\Delta}^H_{g,c}(i,j-1) - \tilde{\Delta}^H_{g,c}(i,j+1)\|,\\ D^V_{i,j} &= \sum_{c\in\{r,or,cy,b\}} \|\tilde{\Delta}^V_{g,c}(i-1,j) - \tilde{\Delta}^V_{g,c}(i+1,j)\|.\end{aligned} \tag{5}$$

Finally, in the step (iv), we obtain the G pixel values at the R pixels by adding the subsampled R band data as:

$$\tilde{G}_{i,j} = \tilde{\Delta}_{g,r}(i,j) + R_{i,j}. \tag{6}$$

The G pixel values at the other pixels are similarly calculated and all G pixel values are merged to compose the full guide G image.

2.3. Interpolation of each subsampled spectral band

After generating the guide G image, we interpolate each subsampled band data by the guided upsampling to obtain interpolated five band images. We utilize the RI [3] again for the guided upsampling. The RI is performed similarly to Fig. 3. The differences are that the tentative estimates are calculated from full guide G image and the bilinear interpolation, instead of the horizontal interpolation, is performed for the interpolation of residuals.

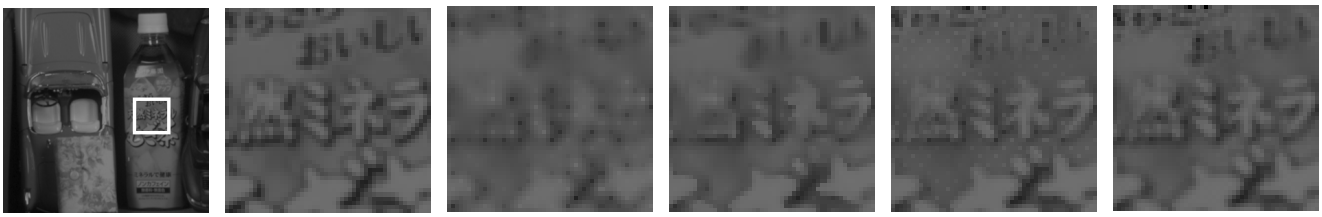

Or band Ground-truth BTES [11] AKU [1] GF [2] Proposed

Fig. 4. Visual comparison of Or band images generated using multispectral demosaicking algorithms.

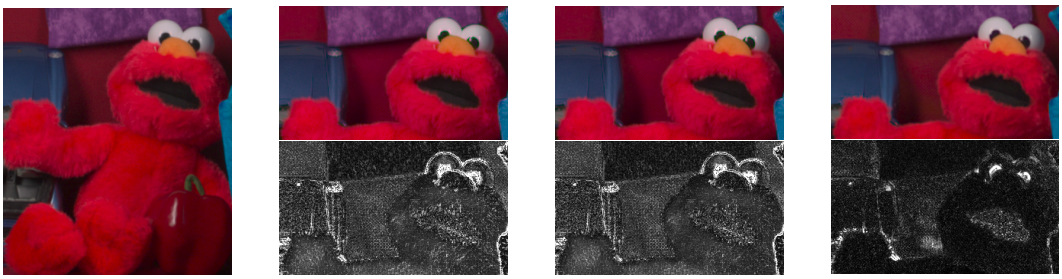

Ground-truth GBTF [21] LPA [22] Proposed

Fig. 5. Visual comparison of sRGB images. The lower half of the image shows the color difference (CIEDE2000 [23]) map, where brighter values represent larger colorimetric errors.

Table 1. The average PSNR and CIEDE2000 [23] of all 16 scenes in the dataset.

	Algorithms	PSNR								CIEDE2000
		R	Or	G	Cy	B	sR	sG	sB	
3band	GBTF [21]	-	-	-	-	-	29.52	39.44	35.53	4.00
	LPA [22]	-	-	-	-	-	30.39	41.24	36.71	3.68
5band	BTES [11]	49.38	45.00	48.60	42.78	44.93	34.46	42.95	36.36	2.91
	AKU [1]	52.19	47.80	48.78	45.38	48.06	38.14	44.20	39.53	2.34
	GF [2]	53.12	51.06	49.61	47.94	48.89	40.75	45.73	40.51	2.06
	Proposed	**54.93**	**52.31**	**51.08**	**49.42**	**49.86**	**42.49**	**47.19**	**41.26**	**1.88**

3. EXPERIMENTAL RESULTS

In experiments, we used five band image dataset (16 scenes) used in [1, 2] as a aground-truth and compared our proposed algorithm with BTES [11], AKU [1], GF [2], GBTF [21], and LPA [22] algorithms. The image size is 1824×1368. The BTES, AKU, and GF are multispectral demosaicking algorithms, while the GBTF and LPA are current state-of-the-art Bayer demosaicking algorithms. For the GBTF and LPA algorithms, the Bayer CFA RAW data was simulated and demosaicked using only R, G, and B bands among the five bands. To compare the five band multispectral imaging with the typical three band RGB imaging in the sRGB domain, we performed spectral reflectance estimation [24] from the demosaicked five band and RGB images respectively, then we converted the reflectances to sRGB images. We used sRGB images converted from the ground-truth five band images as ground-truth sRGB images.

Fig. 4 shows the visual comparison of Or band images generated using the multispectarl demosaicking algorithms. In Fig. 4, our proposed algorithm can sharply generate the image without severe zipper artifacts appeared in the GF algorithm. Fig. 5 shows the visual comparison of sRGB images generated using the Bayer and our proposed demosaicking algorithms. The lower half of the image shows the color difference (CIEDE2000 [23]) map, where brighter values represent larger colorimetric errors. In Fig. 5, our proposed algorithm can accurately reproduce the red color of the toy. Table 1 shows the average PSNR and CIEDE2000 of all 16 scenes in the dataset. In Table 1, our proposed algorithm outperforms existing algorithms in both PSNR and CIEDE2000.

4. CONCLUSION

In this paper, we proposed a novel multispectral demosaicking algorithm. We utilize multispectral correlations and recently proposed RI for generating an effective guide G image, which is used to interpolate the subsampled spectral data by the framework of guided upsampling. We also utilize the RI as guided upsampling algorithm. Experimental results demonstrate that our proposed algorithm outperforms existing algorithms in both visual and quantitative comparisons.

5. REFERENCES

[1] Y. Monno, M. Tanaka, and M. Okutomi, "Multispectral demosaicking using adaptive kernel upsampling," *Proc. of IEEE Int. Conf. on Image Processing (ICIP)*, pp. 3218–3221, 2011.

[2] Y. Monno, M. Tanaka, and M. Okutomi, "Multispectral demosaicking using guided filter," *Proc. of SPIE*, vol. 8299, pp. 82990O–1–82990O–7, 2012.

[3] D. Kiku, Y. Monno, M. Tanaka, and M. Okutomi, "Residual interpolation for color image demosaicking," *Proc. of IEEE Int. Conf. on Image Processing (ICIP)*, pp. 2304–2308, 2013.

[4] J. Park, M. Lee, M. D. Grossberg, and S. K. Nayar, "Multispectral imaging using multiplexed illumination," *Proc. of IEEE Int. Conf. on Computer Vision (ICCV)*, pp. 1–8, 2007.

[5] S. Han, I. Sato, T. Okabe, and Y. Sato, "Fast spectral reflectance recovery using DLP projector," *Proc. of Asian Conf. on Computer Vision (ACCV)*, pp. 318–330, 2010.

[6] X. Cao, H. Du, X. Tong, Q. Dai, and S. Lin, "A prism-mask system for multispectral video acquisition," *IEEE Trans. on Pattern Analysis and Machine Intelligence*, vol. 33, no. 12, pp. 2423–2435, 2011.

[7] H. Fukuda, T. Uchiyama, H. Haneishi, M. Yamaguchi, and N. Ohyama, "Development of 16-bands multispectral image archiving system," *Proc. of SPIE*, vol. 5667, pp. 136–145, 2005.

[8] K. Ohsawa, T. Ajito, H. Fukuda, Y. Komiya, H. Haneishi, M. Yamaguchi, and N. Ohyama, "Six-band HDTV camera system for spectrum-based color reproduction," *Journal of Imaging Science and Technology*, vol. 48, no. 2, pp. 85–92, 2004.

[9] R. Habel, M. Kudenov, and M. Wimmer, "Practical spectral photography," *Computer Graphics Forum*, vol. 31, no. 2, pp. 449–458, 2012.

[10] L. Miao and H. Qi, "The design and evaluation of a generic method for generating mosaicked multispectral filter arrays," *IEEE Trans. on Image Processing*, vol. 15, no. 9, pp. 2780–2791, 2006.

[11] L. Miao, H. Qi, R. Ramanath, and W. E. Snyder, "Binary tree-based generic demosaicking algorithm for multispectral filter arrays," *IEEE Trans. on Image Processing*, vol. 15, no. 11, pp. 3550–3558, 2006.

[12] J. Brauers and T. Aach, "A color filter array based multispectral camera," *12. Workshop Farbbildverarbeitung*, 2006.

[13] Y. Monno, T. Kitao, M. Tanaka, and M. Okutomi, "Optimal spectral sensitivity functions for a single-camera one-shot multispectral imaging system," *Proc. of IEEE Int. Conf. on Image Processing (ICIP)*, pp. 2137–2140, 2012.

[14] Y. Monno, M. Tanaka, and M. Okutomi, "Direct spatio-spectral datacube reconstruction from raw data using a spatially adaptive spatio-spectral basis," *Proc. of SPIE*, vol. 8660, pp. 866003–1–866003–8, 2013.

[15] R. Shrestha, J. Y. Hardeberg, and R. Khan, "Spatial arrangement of color filter array for multispectral image acquisition," *Proc. of SPIE*, vol. 7875, pp. 787503, 2011.

[16] B. K. Gunturk, J. Glotzbach, Y. Altunbasak, R. W. Schafer, and R. M. Mersereau, "Demosaicking:color filter array interpolation," *IEEE Signal Processing Magazine*, vol. 22, pp. 44–54, 2005.

[17] X. Li, B. Gunturk, and L. Zhang, "Image demosaicing: a systematic survey," *Proc. of SPIE*, vol. 6822, pp. 68221J–68221J–15, 2008.

[18] B. Bayer, "Color imaging array," *U.S. Patent 3971065*, 1976.

[19] J. Kopf, M. F. Cohen, D. Lischinski, and M. Uyttendaele, "Joint bilateral upsampling," *ACM Trans. on Graphics*, vol. 26(3), no. 96, 2007.

[20] K. He, J. Sun, and X. Tang, "Guided image filtering," *Proc. of the 11th European Conf. on Computer Vision (ECCV)*, vol. 6311, pp. 1–14, 2010.

[21] I. Pekkucuksen and Y. Altunbasak, "Gradient based threshold free color filter array interpolation," *Proc. of IEEE Int. Conf. on Image Processing (ICIP)*, pp. 137–140, 2010.

[22] D. Paliy, V. Katkovnik, R. Bilcu, S. Alenius, and K. Egiazarian, "Spatially adaptive color filter array interpolation for noiseless and noisy data," *Int. Journal of Imaging Systems and Technology*, vol. 17, no. 3, pp. 105–122, 2007.

[23] G. Sharma, W. Wu, and E. N. Dalal, "The CIEDE2000 color-difference formula: Implementation notes, supplementary test data, and mathematical observations," *Color Research and Application*, vol. 30, no. 1, pp. 21–30, 2005.

[24] Y. Murakami, K. Fukura, M. Yamaguchi, and N. Ohyama, "Color reproduction from low-SNR multispectral images using spatio-spectral wiener estimation," *Optics Express*, vol. 16, no. 6, pp. 4106–4120, 2008.